Original article

Nuclear Medicine Communications

Is computed tomography attenuation correction more efficient than gated single photon emission computed tomography analysis in improving the diagnostic performance of myocardial perfusion imaging in patients with low prevalence of ischemic heart disease?

Meriem Benkiran[a], Denis Mariano-Goulart[a], Aurélie Bourdon[a], Louis Sibille[b] and Fayçal Ben Bouallègue[a]

Objective **The purpose of this study was to compare computed tomography (CT)-based attenuation correction (AC) using a hybrid single photon emission computed tomography (SPECT)-CT system and quantitative analysis of wall thickening using gated SPECT with regard to the diagnostic accuracy of myocardial perfusion imaging.**

Materials and methods **We prospectively included 70 patients with low prevalence of acute coronary artery disease who underwent a myocardial stress–rest SPECT study. Interpretation was based on supine nongated SPECT data with (AC) or without (NC) CT-based attenuation correction, and on gated SPECT data without attenuation correction (GNC). The scintigraphic diagnosis was obtained using standard automated quantitative analysis software and compared with a 23 ± 14 months' clinical follow-up for 57 patients or with the results of a coronary angiography for 13 patients.**

Results **The sensitivity, specificity, and overall accuracy were, respectively, 77, 60, and 63% for NC SPECT, 67, 81, and 79% for AC SPECT, and 69, 98, and 93% for GNC SPECT. The initial diagnosis was modified in about one-third of the cases for both AC and GNC, this rate being independent of any clinical parameter (including BMI) except sex (two to four times more artifact correction in men).**

Conclusion **Its widespread availability, cost effectiveness, safety in terms of radiation exposure, and ability to significantly improve myocardial perfusion imaging specificity and accuracy make gated SPECT a self-sufficient modality for coronary artery disease screening and follow-up, whereas CT-AC should be discussed on a case-by-case basis.** ***Nucl Med Commun*** **36:69–77 © 2014 Wolters Kluwer Health | Lippincott Williams & Wilkins.**

Nuclear Medicine Communications 2015, **36**:69–77

Keywords: attenuation correction, gated single photon emission computed tomography, myocardial perfusion imaging, single photon emission computed tomography-computed tomography, systolic wall thickening

[a]Nuclear Medicine Department, Lapeyronie University Hospital, Montpellier Cedex 5 and [b]Nuclear Medicine Department, Caremeau University Hospital, Nîmes, France

Correspondence to Denis Mariano-Goulart, PhD, Nuclear Medicine Department, Lapeyronie University Hospital, 371, Av Doyen Gaston Giraud, 34295 Montpellier Cedex 5, France
Tel: +33 467 338 598; fax: +33 467 338 465;
e-mail: d-mariano_goulart@chu-montpellier.fr

Received 30 July 2014 **Revised** 26 August 2014 **Accepted** 26 August 2014

Introduction

Myocardial perfusion imaging (MPI) using single photon emission computed tomography (SPECT) has been well established for the diagnosis and risk stratification of coronary artery disease (CAD). However, the full clinical potential of MPI has not been realized because of numerous factors producing artifacts that degrade image quality and result in misinterpretation of the results [1]. Motion and nonuniform photon attenuation in the chest can cause significant artifacts. Especially for supine SPECT acquisitions, this may produce a relative count decrease in the inferior wall as a result of breast or diaphragmatic attenuation or motion [2]. Today, the most widely used attenuation correction (AC) instrumentation utilizes single-slice X-ray computed tomography (CT-AC) for acquisition of transmission maps [3,4]. Several reports on the use of AC in MPI have shown discordant results and its utility in routine clinical practice is still debated [3,5,6].

Moreover, even if the contribution of low-dose CT scans to the total radiation dose to patients undergoing SPECT-CT examinations is low compared with diagnostic CT [7], addition of low-dose CT to myocardial nuclear medicine procedures increases the radiation dose to the patient, with an effective dose due to CT similar to the effective dose of ^{99m}Tc radiopharmaceuticals [8].

During the last two decades, the analysis of wall thickening using gated studies has been routinely used to identify attenuation artifacts as myocardial segments with nonreversible hypoactivity and normal wall motion and thickening [9], and thus the analysis of gated studies may be an alternative to the use of external X-ray sources for attenuation identification.

0143-3636 © 2014 Wolters Kluwer Health | Lippincott Williams & Wilkins

DOI: 10.1097/MNM.0000000000000218

Table 1 Clinical and anthropometric characteristics of the study population

Men [*n* (%)]	45 (64)
Women [*n* (%)]	25 (36)
Sex ratio	1.8
Age (years)	61 ± 11
BMI (kg/m^2)	27 ± 4
Abdominal perimeter (cm)	102 ± 13
Thoracic perimeter (cm)	103 ± 10
Heart rate during stress acquisition (/min)	84 ± 18
Respiratory rate during stress acquisition (/min)	19 ± 4

The aim of the present study was to evaluate the consequences of CT-AC and/or wall thickening analysis on the diagnostic performance of MPI in routine clinical settings.

Materials and methods

Patients

We prospectively included 70 patients (25 women and 45 men) referred to the Nuclear Medicine Department at Lapeyronie University Hospital, Montpellier, France, from November 2009 to March 2010. Patients were recruited from those scheduled for routine stress–rest myocardial perfusion SPECT for suspected or known CAD. The patients were aged 61 ± 11 years (range 36–83 years). The clinical and anthropometric characteristics of the study population are summarized in Table 1. The reason for myocardial SPECT was CAD screening for 49 (70%) patients, among whom 30 (43%) had cardiovascular risk factors and 19 (27%) had clinical symptoms (angina pectoris), and CAD control for 21 (30%) patients. Table 2 lists the cardiovascular risk factors in decreasing order of prevalence in the study population.

Study protocol

The study protocol was approved by the local ethics committee (Comité de protection des Personnes Sud Méditerrannée IV, Montpellier University Hospital, under the reference Q-2014-05-06) and all patients gave their oral consent. Patients without contraindication ($n = 62$, 89%) were asked to stop taking nitrates and calcium antagonists at least 24 h before and β-blockers at least 48 h before MPI. Eight patients addressed for CAD control underwent the stress test under β-blocker medication. Patients were also asked to avoid caffeine, drugs, and dipyridamole for 24 h before the study. The stress test was conducted on a treadmill according to the Bruce protocol (30 W increment each 3 min) with slow intravenous administration of 0.56 mg/kg dipyridamole over 4 min in patients without contraindication ($n = 61$, 87%). Seven (10%) patients suffering from asthma or chronic obstructive pulmonary disease underwent the stress test without dipyridamole injection. Two (3%) patients who were not able to produce an effort underwent only a pharmacological stress test. Dipyridamole was injected at peak stress, and exercise was continued for 60 more seconds. The mean heart rate at peak stress was 81 ± 13% of the theoretical maximum heart rate for a load of 84 ± 33 W. ^{99m}Tc-tetrofosmin (Myoview; GE Healthcare, Little Chalfont, UK) was used for both stress and rest MPI in all 70 patients. Sixty-seven patients underwent a 1-day protocol including a stress test followed by a rest test 3 h later if the stress test was positive. The injected dose was 3.7 MBq/kg for the stress imaging (mean 278 MBq, range 249–370 MBq) and 11 MBq/kg for the rest imaging (mean 762 MBq, range 724–876 MBq). Three patients weighing more than 100 kg underwent a 2-day protocol (stress test day 1, rest test day 2). The injected dose was 11 MBq/kg for both stress imaging (mean 762 MBq, range 718–830 MBq) and rest imaging (mean 791 MBq, range 751–842 MBq). Stress images were acquired 10 min after tetrofosmin injection, whereas rest images were acquired 15–30 min after tetrofosmin injection.

Table 2 Cardiovascular risk factors in the study population

Man older than 50 or Woman older than 60 [*n* (%)]	59 (84)
Hypertension (≥140/90 mmHg or medication) [*n* (%)]	31 (44)
Dyslipidemia (medication or LDL > 1.3 and HDL < 0.6 g/l) [*n* (%)]	29 (41)
Treated type 2 diabetes [*n* (%)]	25 (36)
Cigarette smoking [*n* (%)]	21 (30)
Personal history of CAD [*n* (%)]	21 (30)
Obesity (BMI ≥ 30) [*n* (%)]	18 (26)
Familial history of CAD [*n* (%)]	10 (14)
Number of cardiovascular risk factors	2.5 ± 1.1

CAD, coronary artery disease; HDL, high-density lipoprotein; LDL, low-density lipoprotein.

Data acquisition and reconstruction

The acquisitions were performed using a 90° dual-head gamma camera (Infinia Hawkeye 4; GE Healthcare) with an integrated CT scanner. Projections were recorded with a low-energy high-resolution collimator and a 10% energy window centered on the 140 keV photo-peak of ^{99m}Tc. Scatter correction was achieved using Jaszczak's method with a Compton window at 120 keV ± 5% [10]. SPECT acquisitions were recorded over 180° in a step-and-shoot mode using 30 projections every 6° and 40 s per projection. All acquisitions were performed with the patients in the supine position because the AC software associated with our gamma camera was validated in the supine position. The acquisition matrix size was 64 × 64 pixels and the zoom factor was 1.33 for men and 1.66 for women. Both stress and rest studies were gated using eight time frames per cardiac cycle. Images were reconstructed on a Xeleris workstation (GE Healthcare) using the ordered subset expectation maximization algorithm (10 subsets, two iterations) with and without AC. A 3-min low-dose CT scan (140 keV, 2.5 mAs) was acquired at the end of both stress and rest SPECT acquisitions, with a matrix size of 512 × 512 pixels (pixel spacing 0.83 mm). The images were reoriented into vertical long-axis, horizontal long-axis, and short-axis views, and then interpreted by two nuclear physicians both qualitatively and

semiquantitatively using a 17-segment polar map of the relative uptake (RU) (normalized to the maximal myocardial uptake). Images showing significant digestive activity in contact with the left ventricle (LV) led to a systematic repetition of the acquisitions after 30–45 min.

Data interpretation

Each segment of the polar map was assigned a score depending on its RU: 0 if $RU \geq 70\%$, 1 if $50 \leq RU < 70\%$, 2 if $30 \leq RU < 50\%$, 3 if $10 \leq RU < 30\%$, and 4 if $RU < 10\%$. Summed scores were computed on both stress [summed stress score (SSS)] and rest [summed rest score (SRS)] polar maps as the summed scores over the 17 segments. The summed difference score (SDS) between stress and rest data stood as a measure of perfusion defect reversibility [11]. The diagnosis was established as follows:

$$\begin{aligned} &SSS < 3 : \text{normal} \\ &SSS \geq 3 : \begin{cases} SDS = SSS (\text{i.e., } SRS = 0) : \text{ischemia} \\ SDS < SSS \text{ and } SDS \geq 3 : \text{ischemia, + necrosis.} \\ SDS < 3 : \end{cases} \end{aligned}$$

Regional wall motion and thickening were analyzed on rest images. Wall thickening was evaluated by computing the relative variation in counts per pixel between end-diastole and end-systole. Segmental thickening scores were evaluated using standardized scales provided by the manufacturer. The summed thickening score (STS) was defined as the sum of the segmental scores over the 17 segments. LV ejection fraction and end-diastolic and end-systolic volumes were not taken into consideration.

Three procedures were compared for the diagnosis of CAD:

(1) *NC SPECT*: no AC and no ECG gating. Final diagnosis was made on the basis of the SSS and SDS.
(2) *AC SPECT*: no ECG gating. The reconstructed images were attenuation corrected using the CT acquisition map after checking the automatic registration between CT and SPECT images and manual registration if necessary. Final diagnosis was made on the basis of the SSS and SDS.
(3) *GNC SPECT*: no AC. ECG gating allowed wall motion and thickening assessment. The diagnosis provided by the SSS and SDS was corrected using the STS at rest. An STS of 6 or less led to a revision of the first diagnosis from necrosis to normal, and from ischemia + necrosis to ischemia.

Definitive diagnosis

Definitive diagnosis was made either by a coronary angiography performed within 8 ± 6 months after MPI (13 patients, 19%) or by ECG, echocardiography, and clinical follow-up (limited to 36 months) over 23 ± 14 months (57 patients, 81%). To stick to routine clinical settings, as well as for evident ethical considerations, coronary angiography was performed only in patients with a positive MPI (i.e. with a reversible perfusion defect standing for a myocardial ischemia, as defined in the previous section).

Results

Definitive diagnosis

Fifty-seven (81%) patients were considered free of CAD, whereas 13 (19%) patients were diagnosed with CAD: two (3%) patients were diagnosed with myocardial ischemia, eight (11%) with myocardial necrosis, and three (4%) with necrosis associated with ischemia.

Myocardial stress test

The stress test was maximal (i.e. heart rate reached 85% of the theoretical maximum or dipyridamole infusion was used) for all patients but three (96%) and was clinically positive in four patients (two men and two women), electrically positive in five patients (two men and three women), and clinically and electrically positive in two patients (one man and one woman). The stress test was considered positive if the test was clinically or electrically positive (11 patients, 16%). The stress test had a sensitivity of 40%, a specificity of 85%, and an overall accuracy of 81%.

Myocardial perfusion imaging

Automatic segmentation of the LV was systematically controlled and validated by two experienced nuclear medicine physicians, without showing significant discrepancy. Table 3 summarizes the diagnostic performances of NC, GNC, and AC SPECT.

Figure 1 details the false-positive results (among the patients free of CAD) in terms of false necrosis and/or false ischemia. Figure 2 details the final diagnoses in

Table 3 Performances of NC, GNC, and AC SPECT for the diagnosis of coronary artery disease (value and 95% confidence interval)

	NC	GNC		AC	
Sensitivity	77% (54–100%)	69% (44–94%)	NS	67% (41–92%)	NS
Specificity	60% (47–72%)	98% (95–100%)	$P < 10^{-8}$	81% (71–91%)	$P = 0.01$
Accuracy	63% (52–74%)	93% (87–99%)	$P < 10^{-5}$	79% (69–88%)	$P = 0.04$
Positive likelihood ratio	1.9	39	NS	3.5	NS
Negative likelihood ratio	0.39	0.31	NS	0.41	NS

P-values refer to the comparison between NC SPECT taken as a reference and either GNC or AC SPECT.
AC, attenuation correction; SPECT, single photon emission computed tomography.

patients with CAD in terms of right diagnosis, missed necrosis, and missed ischemia. AC SPECT also gave a false-positive result among the patients with CAD by detecting a false ischemia in a patient with known myocardial necrosis. On using either NC, GNC, or AC SPECT, there were two false negatives related to tri-vessel coronary disease.

Figure 3 shows the change in final diagnosis when passing from NC SPECT to GNC and AC SPECT. Attenuation artifacts were corrected in 23 (33%) patients using wall thickening assessment and in 17 (24%) patients using CT-AC.

An unpaired Student *t*-test did not show significant difference between the overall population and the subpopulation in which an artifact was corrected for the following anthropometric parameters: heart rate during stress, respiratory rate during stress, BMI, waist circumference, chest circumference, and chest-to-waist circumference ratio. Sex was the only physiological determinant as 18 (40%) artifact corrections were performed in men versus five (20%) in women using GNC SPECT (sex ratio = 2), and 15 (33%) artifact corrections were performed in men versus two (8%) in women using AC SPECT (sex ratio = 4).

Figures 4–6 illustrate three cases in the study population. In Fig. 4, GNC and AC images confirm myocardial necrosis. In Fig. 5, GNC and AC images allow for the correction of a fixed perfusion defect. In Fig. 6, GNC allows for the correction of a fixed perfusion defect, whereas AC images induce a false ischemia diagnosis.

Fig. 1

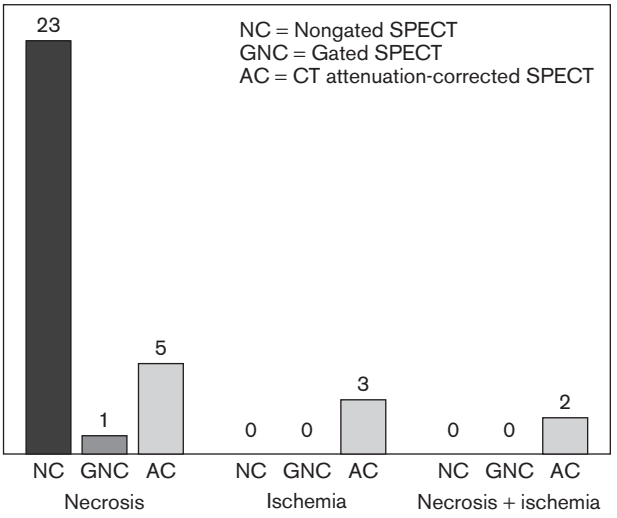

False-positive findings in patients free of coronary artery disease.

Fig. 2

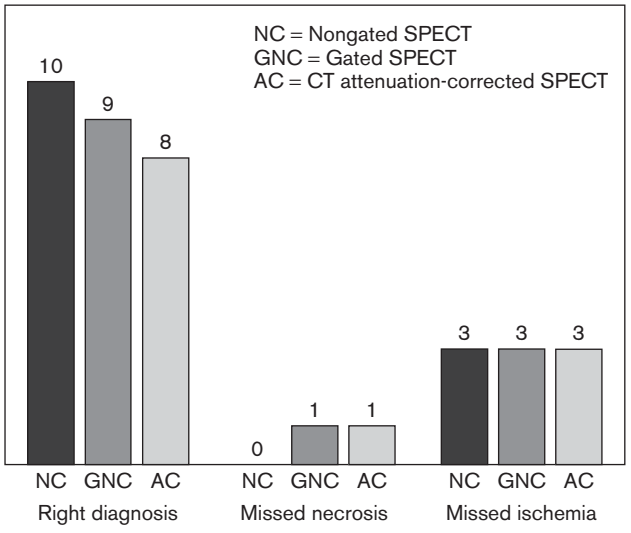

Findings in patients with coronary artery disease.

Dosimetry

The dose length product received by each patient was 124 mGy cm for each transmission (CT) scan with an additional time of 3 min for each acquisition. This dose length product corresponds to an additional effective dose of 2 mSv [12]. For the SPECT acquisitions, the effective dose received by each patient was estimated from the injected activity [13]. On the basis of a whole-body effective dose of 7.5 μSv/MBq for the stress acquisition and 8.5 μSv/MBq for the rest acquisition, the estimated effective dose was 8.6 mSv in average for the 1-day protocol and 12 mSv in average for the 2-day protocol. Thus, for patients who were not overweight (1-day protocol), the effective dose received by a patient during the low-dose CT procedure was equivalent to the dose required for the acquisition of the stress scintigraphic data.

Discussion

In our work, we compared the diagnostic performance of gated SPECT versus CT-AC SPECT in patients with a low prevalence of ischemic heart disease (81% were exempt of CAD). The aim of the study was to evaluate the capacity of CT-based AC and wall motion/thickening analysis to increase MPI specificity while preserving sufficient sensitivity. Photon attenuation within the patient's body is widely recognized as the preponderant physical factor affecting the quantitative accuracy of MPI, leading to potential misinterpretation of perfusion images [14–17]. Several methods have been proposed to correct for attenuation artifacts, including prone imaging [18,19], ECG-gated SPECT, and CT-based AC. AC using CT-derived attenuation maps was first applied in the field of PET imaging [20,21], and has gained popularity over the

Fig. 3

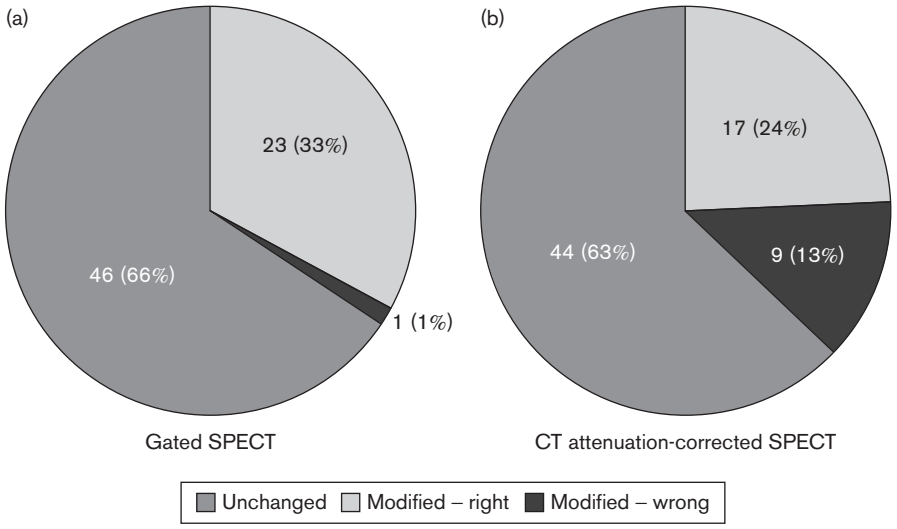

Change in interpretation between (a) NC and GNC images and (b) NC and AC images.

Fig. 4

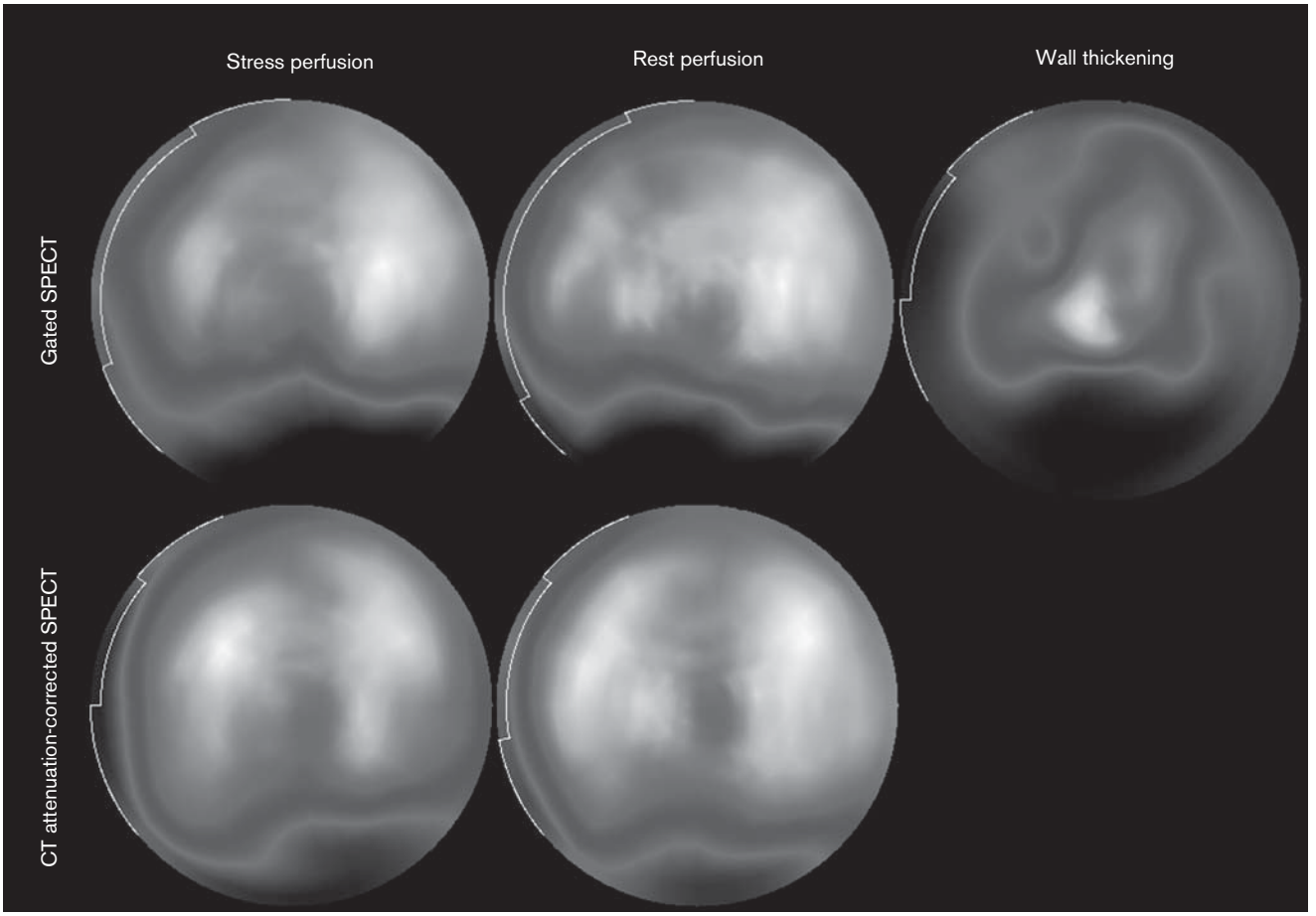

Example of a 74-year-old male patient referred for coronary artery disease control. Noncorrected images (top row) show an inferomediobasal fixed perfusion defect. Altered wall thickening at rest in the same area confirms myocardial necrosis. CT-AC images (bottom row) also show an inferobasal perfusion defect on both stress and rest acquisitions.

Fig. 5

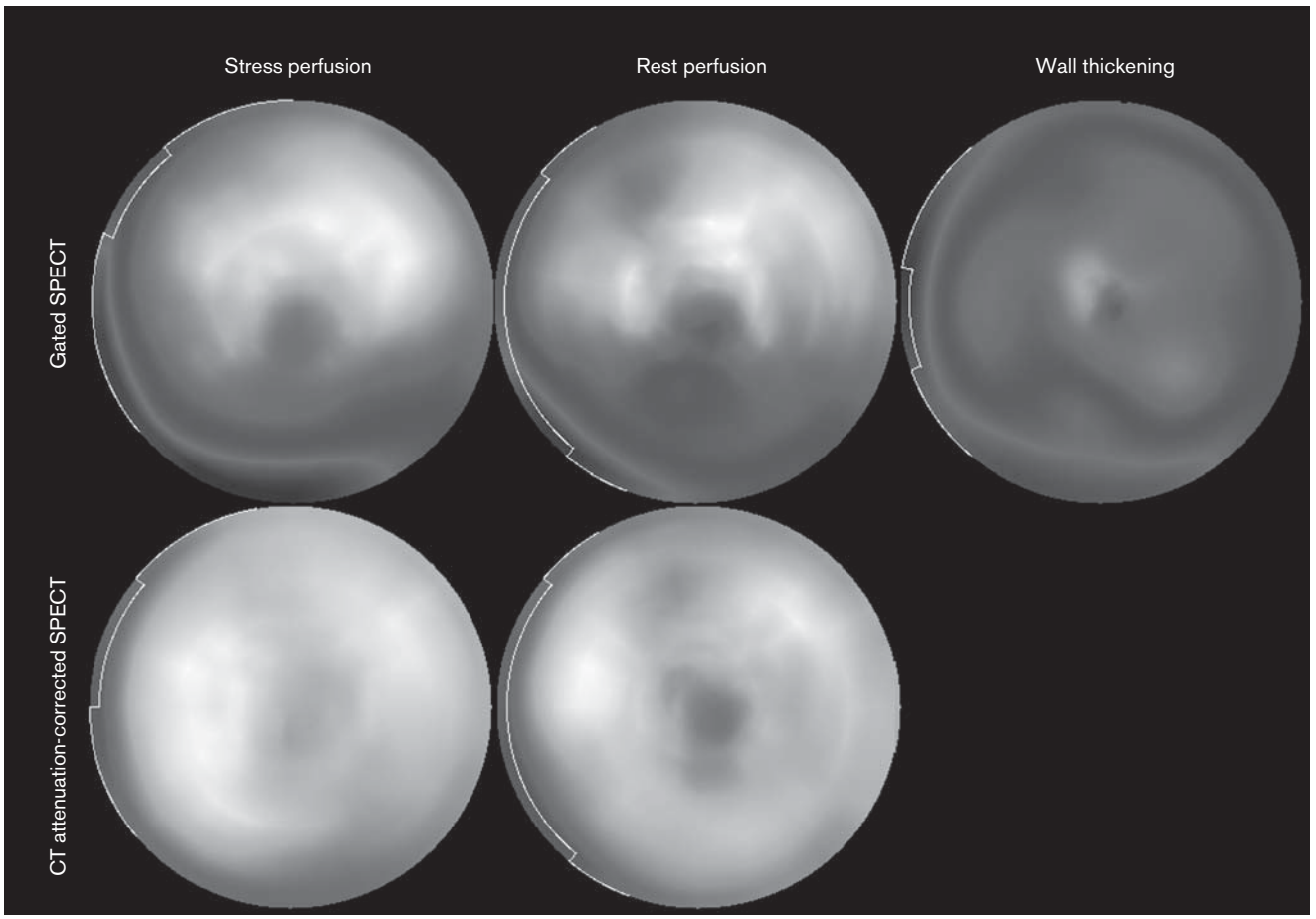

Example of a 57-year-old male patient with dyslipidemia, familial history of coronary artery disease, and HIV infection, referred for coronary artery disease screening. Noncorrected images (top row) show an artifactual inferobasal fixed perfusion defect. Normal wall thickening at rest in the same area allows correcting for the artifact. CT-AC images (bottom row) show uniform tracer distribution on both stress and rest acquisitions and allows correcting for the artifact.

last decades in the field of SPECT imaging as most of the camera manufacturers offer hybrid SPECT-CT systems. Although the use of external sources has been proposed for AC purposes [22], nowadays AC correction factors are usually computed from the CT map [23,24] and integrated in an iterative reconstruction algorithm [16,19]. Although AC SPECT is known to allow better specificity in CAD detection compared with NC SPECT, there is no consensus regarding the relative performances of AC and NC SPECT in terms of sensitivity and overall diagnosis accuracy [3,25–28], and CT-AC quality has been shown to suffer from patient's motion and to induce overcorrections related to misregistration or truncation artifacts [29,30]. Obesity may be considered a natural cause for attenuation artifact, and obese people may be expected to particularly benefit from CT-AC; yet, the many studies on the value of AC myocardial SPECT in the population of overweight patients yielded discordant results [5,31–34].

Systematic use of ECG gating has deeply modified routine myocardial SPECT, allowing the differentiation between CAD and attenuation artifacts in patients showing fixed perfusion abnormalities. A fixed perfusion defect can be regarded as resulting from soft-tissue attenuation if associated with normal LV function, whereas an abnormal LV function will reinforce the diagnosis of myocardial necrosis or stunning. LV function assessment leads to a significant rise in specificity and diagnostic accuracy [9,35–38], has the ability to detect stress-induced abnormalities as in the case of post-ischemic stunning for instance [39,40], and adds prognostic information to myocardial SPECT [41]. Besides, it has been argued by some authors that gated SPECT and CT-AC might have a synergistic impact on the diagnostic accuracy of myocardial SPECT [31,42,43].

In our study, as outlined in Table 3, both AC and GNC SPECT led to improved specificity and diagnostic

Fig. 6

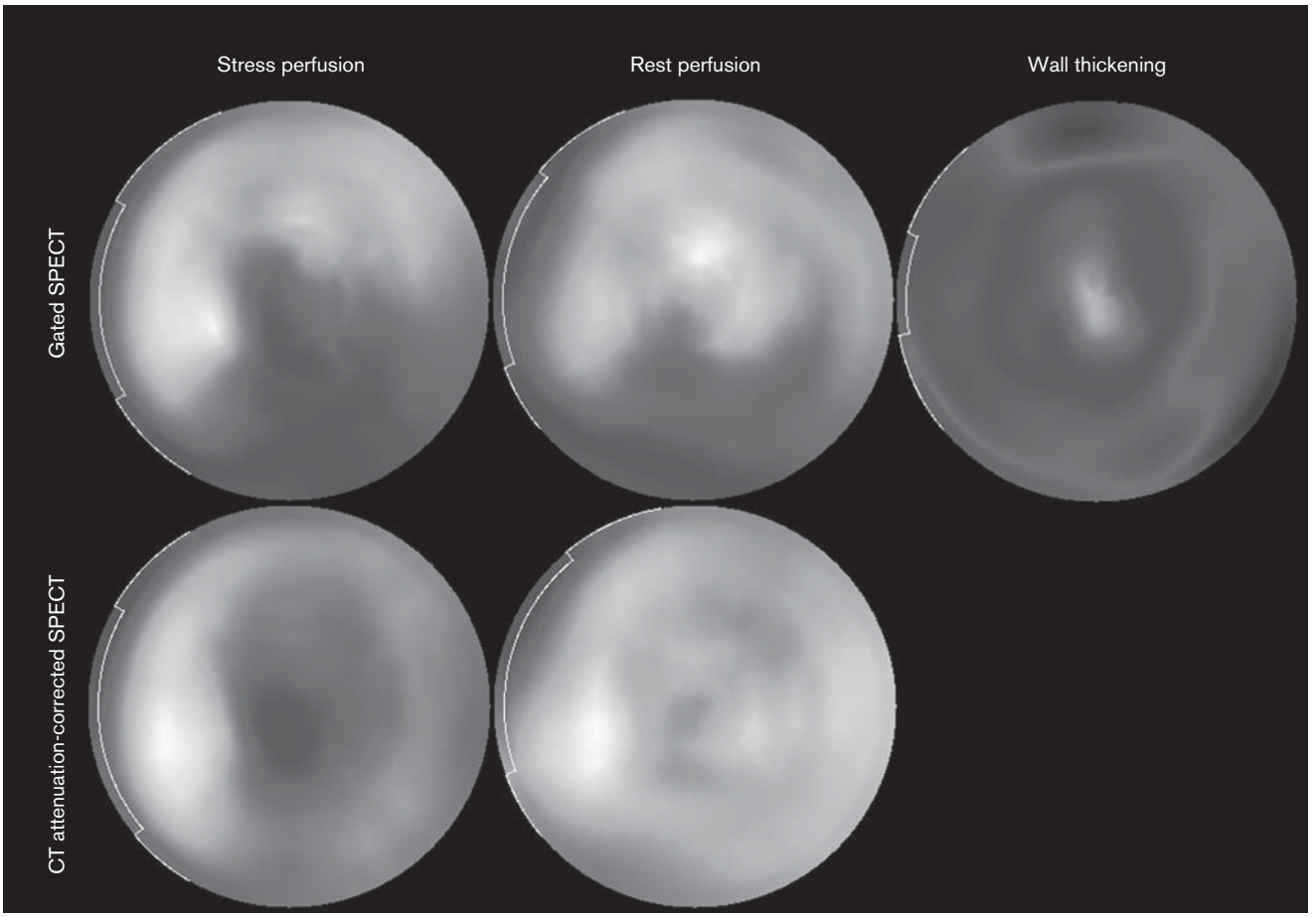

Example of a 60-year-old male patient with diabetes, high blood pressure, dyslipidemia, obesity, and chronic renal failure who was referred for coronary artery disease screening. Noncorrected images (top row) show an artifactual inferolateral fixed perfusion defect. Normal wall thickening at rest in the same area allows correcting for the artifact. CT-AC images (bottom row) show uniform tracer distribution on both stress and rest acquisitions in the inferobasal area but induce a false ischemia diagnosis (reversible apical defect).

accuracy compared with NC SPECT. NC, AC, and GNC showed, respectively, 60, 81, and 98% specificity and 63, 79, and 93% accuracy. The significance of these improvements was, however, undoubtedly higher for GNC than for AC. Sensitivity was similar for the three methods and, although it decreased a little using AC and GNC, no significant difference was found compared with NC SPECT. As shown in Fig. 1, among the 23 patients free of CAD for whom NC SPECT resulted in a false-positive diagnosis of myocardial necrosis, the artifact was corrected for 22 using GNC and for 18 using CT-AC (as for the case exposed in Fig. 5). Gated SPECT did not induce any additional false positives, whereas CT-AC led to five additional false-positive diagnoses including myocardial ischemia (as for the case exposed in Fig. 6). These additional false-positive results, likely resulting from CT-AC-specific artifacts as discussed above, led to inappropriate patient management. Regarding the 13 patients with CAD, Fig. 2 indicates that the diagnostic performances of the three methods were roughly identical. There were two patients with balanced three-vessel CAD that was not detected by any of the three methods.

Figure 3 illustrates that, from a global point of view, the final diagnosis remained unchanged in about two-thirds of the cases using either GNC or AC (as for the case exposed in Fig. 4). Gated SPECT resulted in a diagnostic change for 24 (34%) patients, among which 23 (33%) diagnoses were modified in the right direction. As for AC SPECT, the diagnosis was revised in 26 (37%) cases, among which 17 (24%) were correct and nine (13%) were wrong revisions. It appears that the sole clinical parameter that was significantly linked with correct diagnosis revision was sex (40% of men vs. 20% of women for GNC, and 33% of the men vs. 8% of the women for AC). In particular, neither BMI nor respiratory rate during the

acquisitions was associated with a significant increase in attenuation artifact correction, be it using CT-AC or wall thickening assessment. This higher rate of artifact correction in male patients was likely due to a higher diaphragmatic attenuation in men when undergoing imaging in the supine position.

Although available on most of the contemporary imaging systems, CT-AC has not become, to date, routine practice in myocardial SPECT, mainly because of acquisition and processing time. The constant effort to reduce patients' radiation exposure also accounts for the unwillingness to generalize CT-AC procedures. Various alternative protocols have been proposed in an attempt to reduce the incidence of false-positive findings in MPI [44–46]. During the past two decades, ECG-gated cardiac SPECT has become part of mainstream clinical practice for the evaluation of patients with known or suspected CAD. It does not imply incremental radiation exposure, nor does it require additional acquisition time when heart rate is regular. Moreover, analysis of systolic wall thickening is not concerned with registration issues [47]. Our results tend to support the fact that gated SPECT is more efficient than CT-AC in detecting artifactual false positives and hence in improving the specificity and diagnostic accuracy of MPI, without significant reduction in sensitivity. No correlation was found between artifact correction and any of the studied anthropometric characteristics, including BMI and respiratory rate. This latest consideration might corroborate the hypothesis that attenuation is not the one and only cause for false-positive findings [48].

Conclusion

According to our results, both CT-AC and gated SPECT allow significant gains in terms of specificity and diagnostic accuracy compared with NC SPECT, while preserving similar sensitivity, in patients with low prevalence of CAD. Gated SPECT, however, provided more significant improvements compared with CT-AC. The rate of rectified diagnoses was approximately one-third using either AC or GNC and was not correlated with any clinical parameter except sex (two to four times more artifact corrections in men than in women). In our study, GNC did not induce any additional false-positive result compared with NC, whereas AC led to five false ischemia results with subsequent inadequate patient management. Its widespread availability, cost effectiveness, safety in terms of radiation exposure, efficiency in rectifying most of the false-positive results (not only those related to body attenuation), and ability to provide prognostic information should encourage nuclear medicine physicians to consider gated SPECT as a self-sufficient modality for CAD screening and follow-up. As for CT-AC, it should be discussed on a case-by-case basis and performed only when some doubt remains after gated SPECT analysis, or if gated SPECT conclusions are not consistent with the clinical context.

Acknowledgements

Conflicts of interest

There are no conflicts of interest.

References

1 Mowatt G, Vale L, Brazzelli M, Hernandez R, Murray A, Scott N, *et al.* Systematic review of the effectiveness and cost-effectiveness, and economic evaluation, of myocardial perfusion scintigraphy for the diagnosis and management of angina and myocardial infarction. *Health Technol Assess* 2004; **8**:iii–iv, 1–207.

2 Vidal R, Buvat I, Darcourt J, Migneco O, Desvignes P, Baudouy M, Bussière F. Impact of attenuation correction by simultaneous emission/transmission tomography on visual assessment of ^{201}Tl myocardial perfusion images. *J Nucl Med* 1999; **40**:1301–1309.

3 Genovesi D, Giorgetti A, Gimelli A, Kusch A, D'Aragona Tagliavia I, Casagranda M, *et al.* Impact of attenuation correction and gated acquisition in SPECT myocardial perfusion imaging: results of the multicentre SPAG (SPECT Attenuation Correction vs Gated) study. *Eur J Nucl Med Mol Imaging* 2011; **38**:1890–1898.

4 Patton JA, Townsend DW, Hutton BF. Hybrid imaging technology: from dreams and vision to clinical devices. *Semin Nucl Med* 2009; **39**:247–263.

5 Thompson RC, Heller GV, Johnson LL, Case JA, Cullom SJ, Garcia EV, *et al.* Value of attenuation correction on ECG-gated SPECT myocardial perfusion imaging related to body mass index. *J Nucl Cardiol* 2005; **12**:195–202.

6 Garcia EV. SPECT attenuation correction: an essential tool to realize nuclear cardiology's manifest destiny. *J Nucl Cardiol* 2007; **14**:16–24.

7 Montes C, Tamayo P, Hernandez J, Gomez-Caminero F, García S, Martín C, Rosero A. Estimation of the total effective dose from low-dose CT scans and radiopharmaceutical administrations delivered to patients undergoing SPECT/CT explorations. *Ann Nucl Med* 2013; **27**:610–617.

8 Sharma P, Sharma S, Ballal S, Bal C, Malhotra A, Kumar R. SPECT-CT in routine clinical practice: increase in patient radiation dose compared with SPECT alone. *Nucl Med Commun* 2012; **33**:926–932.

9 Sciagrà R. The expanding role of left ventricular functional assessment using gated myocardial perfusion SPECT: the supporting actor is stealing the scene. *Eur J Nucl Med Mol Imaging* 2007; **34**:1107–1122.

10 Jaszczak RJ, Floyd CE, Coleman RE. Scatter compensation techniques for SPECT. *IEEE Trans Nucl Sci* 1985; **32**:786–793.

11 Hesse B, Tägil K, Cuocolo A, Anagnostopoulos C, Bardiés M, Bax J, *et al.* EANM/ESC Group. EANM/ESC procedural guidelines for myocardial perfusion imaging in nuclear cardiology. *Eur J Nucl Med Mol Imaging* 2005; **32**:855–897.

12 Huda W, Ogden KM, Khorasani MR. Converting dose–length product to effective dose at CT. *Radiology* 2008; **248**:995–1003.

13 Johansson L, Mattsson S, Nosslin B, Leide-Svegborn S. Effective dose from radiopharmaceuticals. *Eur J Nucl Med* 1992; **19**:933–938.

14 DePuey EG III. How to detect and avoid myocardial perfusion SPECT artifacts. *J Nucl Med* 1994; **35**:699–702.

15 King MA, Tsui BM, Pan TS. Attenuation compensation for cardiac single-photon emission computed tomographic imaging: Part 1. Impact of attenuation and methods of estimating attenuation maps. *J Nucl Cardiol* 1995; **2**:513–524.

16 King MA, Tsui BM, Pan TS, Glick SJ, Soares EJ. Attenuation compensation for cardiac single-photon emission computed tomographic imaging: Part 2. Attenuation compensation algorithms. *J Nucl Cardiol* 1996; **3**:55–64.

17 Bateman TM, Cullom SJ. Attenuation correction single-photon emission computed tomography myocardial perfusion imaging. *Semin Nucl Med* 2005; **35**:37–51.

18 Johnstone DE, Wackers FJ, Berger HJ, Hoffer PB, Kelley MJ, Gottschalk A, Zaret BL. Effect of patient positioning on left lateral thallium-201 myocardial images. *J Nucl Med* 1979; **20**:183–188.

19 Singh B, Bateman TM, Case JA, Heller G. Attenuation artifact, attenuation correction, and the future of myocardial perfusion SPECT. *J Nucl Cardiol* 2007; **14**:153–164.

20 Bailey DL. Transmission scanning in emission tomography. *Eur J Nucl Med* 1998; **25**:774–787.

21 Zaidi H, Hasegawa B. Determination of the attenuation map in emission tomography. *J Nucl Med* 2003; **44**:291–315.

22 Miles J, Cullom SJ, Case JA. An introduction to attenuation correction. *J Nucl Cardiol* 1999; **6**:449–457.
23 Fleming JS. A technique for using CT images in attenuation correction and quantification in SPECT. *Nucl Med Commun* 1989; **10**:83–97.
24 Bacharach SL, Buvat I. Attenuation correction in cardiac positron emission tomography and single-photon emission computed tomography. *J Nucl Cardiol* 1995; **2**:246–255.
25 Prvulovich EM, Lonn AH, Bomanji JB, Jarritt PH, Ell PJ. Effect of attenuation correction on myocardial thallium-201 distribution in patients with a low likelihood of coronary artery disease. *Eur J Nucl Med* 1997; **24**:266–275.
26 Gallowitsch HJ, Sykora J, Mikosch P, Kresnik E, Unterweger O, Molnar M, *et al.* Attenuation-corrected thallium-201 single-photon emission tomography using a gadolinium-153 moving line source: clinical value and the impact of attenuation correction on the extent and severity of perfusion abnormalities. *Eur J Nucl Med* 1998; **25**:220–228.
27 Hendel RC, Berman DS, Cullom SJ, Follansbee W, Heller GV, Kiat H, *et al.* Multicenter clinical trial to evaluate the efficacy of correction for photon attenuation and scatter in SPECT myocardial perfusion imaging. *Circulation* 1999; **99**:2742–2749.
28 Sharma P, Patel CD, Karunanithi S, Maharjan S, Malhotra A. Comparative accuracy of CT attenuation-corrected and non-attenuation-corrected SPECT myocardial perfusion imaging. *Clin Nucl Med* 2012; **37**:332–338.
29 Cahill J, Kritzman J, Ficaro E, Corbett J. False positive CT based attenuation corrected SPECT myocardial perfusion studies – contributing factors. *J Nucl Med* 2007; **48 (Suppl 2)**:104P.
30 Germano G, Slomka PJ, Berman DS. Attenuation correction in cardiac SPECT: the boy who cried wolf. *J Nucl Cardiol* 2007; **14**:25–35.
31 Heller GV, Bateman TM, Johnson LL, Cullom SJ, Case JA, Galt JR, *et al.* Clinical value of attenuation correction in stress-only Tc-99m sestamibi SPECT imaging. *J Nucl Cardiol* 2004; **11**:273–281.
32 Grossman GB, Garcia EV, Bateman TM, Heller GV, Johnson LL, Folks RD, *et al.* Quantitative Tc-99m sestamibi attenuation-corrected SPECT: development and multicenter trial validation of myocardial perfusion stress gender-independent normal database in an obese population. *J Nucl Cardiol* 2004; **11**:263–272.
33 Wolak A, Slomka PJ, Fish MB, Lorenzo S, Berman DS, Germano G. Quantitative diagnostic performance of myocardial perfusion SPECT with attenuation correction in women. *J Nucl Med* 2008; **49**:915–922.
34 Xu Y, Fish M, Gerlach J, Lemley M, Berman DS, Germano G, Slomka PJ. Combined quantitative analysis of attenuation corrected and non-corrected myocardial perfusion SPECT: method development and clinical validation. *J Nucl Cardiol* 2010; **17**:591–599.
35 DePuey EG, Rozanski A. Using gated technetium-99m-sestamibi SPECT to characterize fixed myocardial defects as infarct or artifact. *J Nucl Med* 1995; **36**:952–955.
36 Smanio PE, Watson DD, Segalla DL, Vinson EL, Smith WH, Beller GA. Value of gating of technetium-99m sestamibi single-photon emission computed tomographic imaging. *J Am Coll Cardiol* 1997; **30**:1687–1692.
37 Fleischmann S, Koepfli P, Namdar M, Wyss CA, Jenni R, Kaufmann PA. Gated (99m)Tc-tetrofosmin SPECT for discriminating infarct from artifact in fixed myocardial perfusion defects. *J Nucl Med* 2004; **45**:754–759.
38 Choi JY, Lee KH, Kim SJ, Kim SE, Kim BT, Lee SH, Lee WR. Gating provides improved accuracy for differentiating artifacts from true lesions in equivocal fixed defects on technetium 99m tetrofosmin perfusion SPECT. *J Nucl Cardiol* 1998; **5**:395–401.
39 Chua T, Kiat H, Germano G, Maurer G, van Train K, Friedman J, Berman D. Gated technetium-99m sestamibi for simultaneous assessment of stress myocardial perfusion, postexercise regional ventricular function and myocardial viability. Correlation with echocardiography and rest thallium-201 scintigraphy. *J Am Coll Cardiol* 1994; **23**:1107–1114.
40 Johnson LL, Verdesca SA, Aude WY, Xavier RC, Nott LT, Campanella MW, Germano G. Postischemic stunning can affect left ventricular ejection fraction and regional wall motion on post-stress gated sestamibi tomograms. *J Am Coll Cardiol* 1997; **30**:1641–1648.
41 Travin MI, Heller GV, Johnson LL, Katten D, Ahlberg AW, Isasi CR, *et al.* The prognostic value of ECG-gated SPECT imaging in patients undergoing stress Tc-99m sestamibi myocardial perfusion imaging. *J Nucl Cardiol* 2004; **11**:253–262.
42 Links JM, DePuey EG, Taillefer R, Becker LC. Attenuation correction and gating synergistically improve the diagnostic accuracy of myocardial perfusion SPECT. *J Nucl Cardiol* 2002; **9**:183–187.
43 Taneja S, Mohan HK, Blake GM, Livieratos L, Clarke SE. Synergistic impact of attenuation correction and gating in routine myocardial SPECT reporting: 2 year follow-up study. *Nucl Med Commun* 2008; **29**:390–397.
44 Blagosklonov O, Sabbah A, Verdenet J, Baud M, Cardot JC. Poststress motionlike artifacts caused by the use of a dual-head gamma camera for (201)Tl myocardial SPECT. *J Nucl Med* 2002; **43**:285–291.
45 Liu YH, Lam PT, Sinusas AJ, Wackers FJ. Differential effect of 180 degrees and 360 degrees acquisition orbits on the accuracy of SPECT imaging: quantitative evaluation in phantoms. *J Nucl Med* 2002; **43**:1115–1124.
46 Hayes SW, De Lorenzo A, Hachamovitch R, Dhar SC, Hsu P, Cohen I, *et al.* Prognostic implications of combined prone and supine acquisitions in patients with equivocal or abnormal supine myocardial perfusion SPECT. *J Nucl Med* 2003; **44**:1633–1640.
47 Germano G, Berman D. *Clinical gated cardiac SPECT*. 2nd ed. Oxford: Blackwell Publishing; 2006.
48 Kirch D, Koss J, Bublitz T, Steele P. False-positive findings on myocardial perfusion SPECT. *J Nucl Med* 2004; **45**:1597.